

## AN AIR SPARGING CFD MODEL FOR HEAP BIOLEACHING OF COPPER-SULPHIDE

Martin J. LEAHY<sup>1,2</sup>, M. Philip SCHWARZ<sup>1</sup> and Malcolm R. DAVIDSON<sup>2</sup>

<sup>1</sup>CSIRO Division of Minerals, Clayton, Victoria 3169, AUSTRALIA

<sup>2</sup>Department of Chemical and Biomolecular Engineering, The University of Melbourne,  
 Victoria, 3010, AUSTRALIA

### ABSTRACT

A computational fluid dynamics (CFD) solver CFX is used to implement a steady state model of heap bioleaching of copper-sulphide, which includes air sparging (forced aeration) based on a previous model (Casas *et al.*, 1998) with natural convection. A parameter analysis is performed which shows that the factors important to copper leaching are liquid and air flow rates, and permeability. The ability to control which parts of the bed received the highest extraction as a function of the liquid and air flow rates was established. Sparging is found to increase the oxygen concentration throughout the heap compared to the circumstance with no sparging (natural convection), and consequently improves the copper extraction significantly. The results show that sparging does not provide any better copper extraction for very high heap permeabilities.

### NOMENCLATURE

$a$	heap top half-width, ( $m$ )
$b$	heap bottom half-width, ( $m$ )
$\mathbf{B}$	body force vector, ( $N/m^3$ )
$c$	upper $x$ value of computational domain, ( $m$ )
$C_a$	air concentration, ( $kg/m^3$ )
$C_L$	oxygen concentration in liquid, ( $kg/m^3$ )
$C_{P,L}$	specific heat of liquid, ( $J/kg/K$ )
$d$	upper $y$ value of computational domain, ( $m$ )
$D_a$	air diffusion coefficient, ( $m^2/s$ )
$FPY$	$kg$ pyrite to $kg$ chalcocite leached
$\mathbf{g}$	gravitational constant vector, ( $m/s^2$ )
$G_o$	copper grade, ( $kg\ Cu/kg\ bed$ )
$H$	bed height, ( $m$ )
$\Delta H_{ch}$	chalcocite enthalpy, ( $J/kg$ )
$He$	Henry's law functional
$h_L$	liquid flow enthalpy, ( $J/m/s$ )
$\Delta H_{Py}$	pyrite enthalpy, ( $J/kg$ )
$\Delta H_R$	reaction enthalpy, ( $J/kg$ )
$K$	bed permeability, ( $m^2$ )
$m$	lower $x$ value of sparging inlet, ( $m$ )
$M_{ch}$	molecular weight chalcocite, ( $kg/mol$ )
$M_{ox}$	molecular weight oxygen, ( $kg/mol$ )
$M_{py}$	molecular weight pyrite, ( $kg/mol$ )
$n$	upper $x$ value of sparging inlet, ( $m$ )
$p$	air pressure, ( $N/m^2$ )
$q_L$	liquid flow rate, ( $m/s$ )
$q_{L,0}$	fixed liquid flow rate, ( $m/s$ )
$R$	resistivity due to porous media, ( $kg/m^3/s$ )
$t$	time, ( $s$ )
$T$	air temperature, ( $K$ )
$t^*$	( $\equiv 1/(d\alpha/dt)$ ) characteristic reaction time, ( $days$ )
$T_0$	buoyancy reference temperature, ( $K$ )

$\mathbf{u}$	air velocity, ( $m/s$ )
$V_{in}$	vertical sparged air speed, ( $m/s$ )
$V_M$	maximum bacterial respiration rate, ( $kg\ O_2/bacteria/s$ )
$W_o$	oxygen mass fraction, ( $kg\ O_2/kg\ air$ )
$X$	bacteria concentration, ( $bacteria/m^3$ )
$(x, y)$	two-dimensional spatial coordinate system, ( $m$ )

### Greek

$\alpha$	copper extracted, ( $Cu/Cu(initial)$ )
$\beta$	stoichiometric coefficient ( $kg\ Cu/kg\ O_2$ )
$\gamma$	air thermal expansion coefficient ( $1/K$ )
$\varepsilon$	bed porosity, (void $m^3/total\ m^3$ )
$\lambda$	air thermal conductivity, ( $W/m/K$ )
$\mu_a$	dynamic air viscosity, ( $kg/m/s$ )
$\mu_L$	dynamic liquid viscosity, ( $kg/m/s$ )
$\rho_a$	air density, ( $kg/m^3$ )
$\rho_{a,0}$	air density ( $=\rho_a$ ), ( $kg/m^3$ )
$\rho_b$	bed density, ( $kg/m^3$ )
$\rho_L$	liquid density, ( $kg/m^3$ )

### INTRODUCTION

Heap bioleaching is an important mineral extraction process used in industry for the removal of metals such as copper and gold from low grade ores (Bartlett, 1998). The process is favoured because of the low maintenance and large volume in processing, only requiring the control of acid application, inoculation of bacteria and provisions for supplying sufficient oxygen throughout the heap. The leaching process occurs as a result of infiltration of sulphuric acid into the heap, which forms a film over the ore particles. Oxygen in the air phase reacts chemically with the ferric ions in the acid and copper sulphide in the ore, to produce ferrous ions and copper in solution which flows out of the heap with the liquid. The process occurs in the presence of bacteria, such as *Thiobacillus ferrooxidans*, which convert ferrous ions back into ferric ions. In addition to the infiltration of acid, the ore particles during heap construction are coated with liquid (acid), which is inoculated with bacteria.

There are a number of factors to be accounted for in heap bioleaching modelling, including the liquid and air flow, bacterial action (possibly multiple species), and copper extraction. The chemical reactions of these components (oxygen, liquid, bacteria, copper) are reasonably well known, however reaction rate depends on mass transfer processes, specifically oxygen supply in many cases. In this work we assume the liquid flow behaviour in the heap is uniform, and look at the effect on copper extraction of air flow in the heap under air sparging (forced aeration), for various assumed bacterial concentrations. Without the

use of sparging, oxygen supply to the heap depends on natural convection which occurs when temperatures inside the heap are greater than outside. The onset of such effects has been studied by Lu and Zhang (1997). For large heaps like those used in industry, this does not provide enough oxygen deep within the heap for copper extraction (Bartlett and Prisbrey, 1998). In addition, Casas *et al.* (1998) found that heaps with height and width larger than 10 by 20 metres, respectively, were ineffective in terms of copper recovery due to lack of air flow.

Previous models of air flow in heaps have included natural convection (Casas *et al.*, 1998; Pantelis and Ritchie, 1991, 1992; Pantelis *et al.*, 2002) with the air flow through the bed described by Darcy's Law (Bear, 1972). Of the models mentioned, none has included sparging of air; moreover none has included the full solution of the Navier-Stokes equations, which can become important at high air flow rates, or very high permeabilities. The analysis here uses the N-S equations with a resistance force based on Darcy's Law.

## MODEL DESCRIPTION

### Assumptions

Consider a two dimensional uniform porous medium of trapezoidal shape (see Figure 1) with a given permeability and porosity. In practice the particle size distribution can be widely varying, with regions of different permeability and porosity through the bed. Figure 1 shows the heap in bold, and the computational domain used.

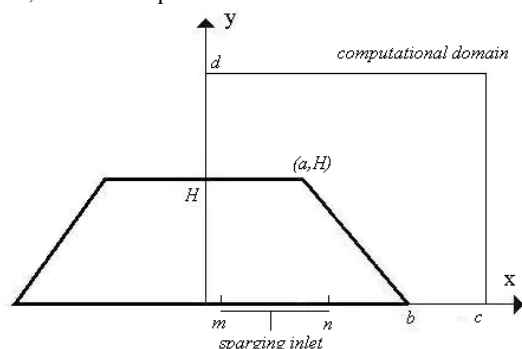


Figure 1: schematic heap

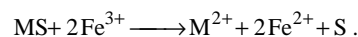
Acid solution is assumed to feed uniformly downward under the influence of gravity, though in practice the solution flow can take tortuous flow paths, with both channelling and liquid stagnant regions, due to heterogeneities and properties of the unsaturated liquid flow (Bartlett, 1998). The liquid is assumed to coat the grains of the heap such that its affect on the pore space available to the gas can be ignored. Due to the large grain size, capillary pressure is neglected in this work and the gas flow is determined from a single-phase, rather than a two-phase calculation. It can be shown that it is a good approximation to assume that the temperature of the air is in local thermodynamic equilibrium with the liquid and ore bed. Consequently, it is sufficient to solve for the heat transport of air, taking into account the heat advected by the liquid.

The bacterial concentration would vary in time and space in practice, but is kept constant in this work for simplicity, however this aspect will be expanded in future work to

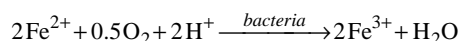
include dynamic and spatially variable kinetics (Monod, temperature, pH), and mobility/attachment via liquid flow.

### Reactions

The ore being considered in this work is composed of pyrite (iron sulphide) and chalcocite (copper sulphide). The reaction of a metal sulphide (MS) in the heap is a two-stage reaction. The solution contains ferric ions ( $Fe^{3+}$ ) that reacts with copper sulphide to produce ferrous ions ( $Fe^{2+}$ ) as



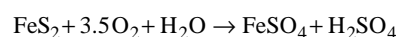
Ferrous ions are re-oxidized to ferric ions in the presence of bacteria (only *T. ferrooxidans* is considered) as



where M is the metal copper or iron, present in chalcocite and pyrite respectively. We follow the approach of Casas *et al.* (1998) who assume the bacteria and oxygen in the liquid are limiting the reaction rate, whilst the ferrous ions are in excess so that  $\alpha$  (copper extracted) can be described by the Michaelis-Menton form

$$\frac{d\alpha}{dt} = \frac{\beta}{\rho_b G_o} X V_M \frac{C_L}{K_M + C_L}, \quad (1)$$

where  $X$ ,  $V_M$ ,  $K_M$  and  $C_L$  are the bacteria concentration, maximum specific respiration rate of bacteria, Michaelis-Menton half growth rate constant and liquid concentration respectively. The overall reactions for chalcocite  $Cu_2S$  and pyrite  $FeS_2$  have the stoichiometries



From these reactions, we can derive the stoichiometric factor  $\beta$ , the mass ratio of copper produced to oxygen consumed as

$$\beta = \frac{M_{Ch} M_{Py}}{2.5 M_{Ox} M_{Py} + 3.5 (FPY) M_{Ox} M_{Ch}}. \quad (2)$$

In (1),  $\rho_b$  and  $G_o$  are the bed density and copper grade respectively, and in (2)  $FPY$  is the ratio of mass of pyrite to the mass of chalcocite leached, which is kept constant in the work, although in practice it will vary in time and cause the copper extraction described in (1) to slow in time. The maximum respiration rate for *T. ferrooxidans* bacteria is given by Casas *et al.* (1998), dependent on temperature as

$$V_M = \frac{6.8 \times 10^{-13} T \exp(-7000/T)}{1 + \exp(236 - 74000/T)}. \quad (3)$$

This relation exhibits a maximum value for temperature around  $37^\circ C$ , and conforms to the temperature range  $4-46^\circ C$  in the literature in which bacteria can survive (Ahonen and Tuovinen, 1989).

The oxygen concentration  $C_a$  is written in terms of oxygen mass fraction  $W_o$  as

$$C_a = \rho_a W_o \quad (4)$$

Henry's law gives the oxygen concentration in the liquid  $C_L$

$$C_L = He C_a \quad (5)$$

where

$$He = -7 \times 10^{-8} (T - 273.15)^3 + 1.55 \times 10^{-5} (T - 273.15)^2 - 1.2 \times 10^{-3} (T - 273.15) + 5.23 \times 10^{-2} \quad (6)$$

by fitting oxygen solubilities in water as a function of temperature (Perry and Green, 1984).

#### Air Flow

The steady state flow occurring in the porous heap is described by the equation of continuity and the steady state N-S equations given by

$$\nabla \cdot \mathbf{u} = 0 \quad (7)$$

$$\rho_a \nabla \cdot (\mathbf{u}\mathbf{u}) = -\nabla p + \mu_a \nabla^2 \mathbf{u} + \mathbf{B} \quad (8)$$

where  $p$ ,  $\mathbf{u}$ ,  $\mathbf{B}$ ,  $\mu_a$  and  $\rho_a$  are the pressure, velocity, body forces, air viscosity and density. The body force  $\mathbf{B}$  accounts for the Darcy resistance to flow in the porous medium and gravity by taking the form

$$\mathbf{B} = -R \mathbf{u} + \rho_a \mathbf{g} \quad (9)$$

where  $\mathbf{g}$  is the gravitational vector and  $R$  is the porous resistivity (Al-Khlaifat and Arastoopour, 1997) given by

$$R = \frac{\varepsilon \mu_a}{K} \quad (10)$$

Here  $\varepsilon$  and  $K$  are the porosity and permeability of the heap respectively. For low flow rates (as in this work), it can be shown equations (8), (9) and (10) represents Darcy flow.

Although the air is not considered compressible, the air density  $\rho_a$  varies due to differences in the air temperature, and induces a buoyancy effect. The Boussinesq approximation is used to describe the air density for the body force terms for  $\rho_a$  in (9) as

$$\rho_a = \rho_{a,0} (1 - \gamma(T - T_0)), \quad (11)$$

where  $\gamma$  is the thermal expansion coefficient of air,  $\rho_{a,0}$  is constant and equal to the air density in atmospheric conditions, and  $T_0$  is the buoyancy reference temperature. The density on the left hand side of (8) is set equal to the atmospheric value, so that the momentum equation is given by

$$\rho_{a,0} \nabla \cdot (\mathbf{u}\mathbf{u}) = -\nabla p + \mu_a \nabla^2 \mathbf{u} - \frac{\varepsilon \mu_a}{K} \mathbf{u} - \rho_{a,0} (1 - \gamma(T - T_0)) \mathbf{g} \quad (12)$$

#### Liquid Flow

The liquid is assumed to flow vertically and to have a negligible effect on the flow of air, except to cool it. A more sophisticated liquid flow model could be included, involving liquid hold-up (Bouffard and Dixon, 2001), or unsaturated liquid flow (Pantelis *et al.*, 2002). However, for the purposes of the air phase modelling in this work, we use a constant liquid velocity within the heap.

#### Energy Balance

The temperature is described by the steady-state heat equation with a source term given by

$$\frac{\partial h_L}{\partial y} - \Delta H_R \frac{\rho_b G_o}{\beta} \frac{d\alpha}{dt} = \lambda \nabla^2 T - \mathbf{u} \nabla \cdot T \quad (13)$$

where  $\lambda$  is the thermal conductivity of air. The first term on the left hand side of (13) represents the heat taken up by the liquid, whilst the second term is the heat produced by the reactions. In (13)  $h_L = -q_L C_{p,L} \rho_L (T - T_{ref})$  where  $C_{p,L}$  is the specific heat of liquid, and  $\Delta H_R$  is the heat of reaction given by Casas *et al.* (1998) as  $\Delta H_R = H_{py} + FPY H_{ch}$ , where  $H_{py}$  and  $H_{ch}$  are the heat of reactions for pyrite and chalcocite respectively.

#### Oxygen Balance

Transport of oxygen in the heap is described by advection and molecular diffusion (we have not included an increased effective diffusion due to porous medium), modified by reactions, and is described by

$$\frac{\rho_b G}{\beta} \frac{d\alpha}{dt} = \rho_a D_a \nabla^2 W_o - \rho_a \nabla \cdot (W_o \mathbf{u}) \quad (14)$$

where  $D_a$  is the diffusion coefficient of air, and the term on the left hand side of (14) is the sink term due to reactions.

#### Boundary Conditions

The conditions imposed at the boundaries of the computational domain (see Figure 1) are as follows;

$$\mathbf{u}(x,0) = (0, V_{in}), \quad T(x,0) = 298K \quad m \leq x \leq n \quad (15)$$

$$\frac{\partial T(x,0)}{\partial y} = 0 \quad 0 \leq x \leq m \quad \text{and} \quad n \leq x \leq c \quad (16)$$

$$\frac{\partial T(0,y)}{\partial x} = 0 \quad (17)$$

$$p(x,d) = 1 \text{ atm for } 0 \leq x \leq c, \quad p(c,y) = 1 \text{ atm for } 0 \leq y \leq d. \quad (18)$$

Several inlet velocities  $V_{in}$  at  $y=0$ ,  $x \in (m, n)$  are used in the results section. We also present the results without sparging, however unlike Casas *et al.* (1998), we do not force the flow to be perpendicular to the heap surface as it enters or leaves. Symmetry of the solution applies around the line  $x=0$  allows the computation domain in Figure 1 to be restricted to the region  $0 \leq x \leq c$ ,  $0 \leq y \leq d$ . The computational domain used was larger than the actual heap (see Figure 1), with pressure boundaries at the outer edges of the computational domain. The resultant flow was such that air leaves the heap and then flows through the rest of the computational domain, so that boundary conditions for the actual heap edges are not required.

#### Numerical Method

The steady state equations (1)-(7), (12)-(18) were solved using CFX4, and the simulations required an orthogonal grid (250 by 250 cells) to avoid instability. The grid used was rectangular and a staircase of computational cells represents the slanted top of the heap. The results for a grid with 125 by 125 cells was found to be insignificantly different to that of 250 by 250 cells. The liquid enthalpy flow in (13) was approximated using upwind differencing to ensure stability, but all spatial derivatives were approximated using central differencing. The results were assumed converged when the normalized residuals were all less than  $1 \times 10^{-3}$ . Liquid was applied evenly across entire exposed boundary of the heap with a given flow velocity  $q_L$ .

## RESULTS

### Parameter Analysis

The concentration of bacteria in the heap, in particular *T. ferrooxidans*, is largely unknown, and it is appropriate to look at the effect of such levels on the temperature, oxygen and hence copper extraction. Hence, the results are split into two parts for low and high bacterial concentrations, with values of  $X=5 \times 10^{13}$  bacteria/m<sup>3</sup> and  $X=5 \times 10^{12}$  bacteria/m<sup>3</sup> respectively. We have not investigated the effect of variation of the *FPY* factor, unlike Casas et al (1998), due to space constraints. In the next two sections the following parameters were used (Table 1). Further parameters and variables are specified where appropriate.

Bed porosity	$\varepsilon=0.3(m^3/m^3)$
Bed height	$H=10(m)$
Top and bottom length	$a=8(m), b=20(m)$
Upper computational domain x, y	$c=10(m), d=25(m)$
Air density	$\rho_a=1.208(kg/m^3)$
Air viscosity	$\mu_a=1.812 \times 10^{-5}(kg/m \cdot s)$
Air diffusion coefficient	$D_a=1.44 \times 10^{-5}(m^2/s)$
Air thermal conductivity	$\lambda=2.88 \times 10^{-2}(W/m \cdot K)$
Air thermal expansion coefficient	$\gamma=3.43 \times 10^{-3}(1/K)$
Liquid specific heat	$C_{p,L}=4000(J/kg \cdot K)$
Relative liquid flow rate	$q_{L,0}=1.4 \times 10^{-6} m/s$
Monod half growth rate constant	$K_m=1 \times 10^{-3}(kg/m^3)$
Heat of reaction for pyrite	$\Delta H_{py}=-1.26 \times 10^7(J/kg)$
Heat of reaction for chalcocite	$\Delta H_{ch}=-6.0 \times 10^6(J/kg)$
Stoichiometric factor	$\beta=0.193370$
Copper grade	$G_o=0.5 \% wt$
FPY	$FPY=5$
Atmospheric oxygen mass fraction	$W_o(atmospheric)=22\%wt$

**Table 1:** parameters for all results.

### Low Bacterial Levels

The results found for relatively low bacterial levels are described in this section, with the constant value  $X=5 \times 10^{12}$  bacteria/m<sup>3</sup>. In Figures 2-5 we see (in order) the 2-D plots (with streamlines) of vectors coloured by speed, and flooded contours of % oxygen mass fraction normalized by atmospheric oxygen mass fraction ( $100 \times W_o/0.22$ ), temperature and % copper extracted ( $\alpha \times 100$ , after 1 year) for a sparging velocity  $V_{in}=1 \times 10^{-4}$  m/s. In Figure 5, the copper extracted after 1 year is calculated by extrapolating linearly from the initial reaction rate. This corresponds to a typical air flow rate used in practice (Bartlett, 1998). The figures show that some natural convection occurs, whilst sparging dominates the air flow. The oxygen mass fraction stays relatively high through out the heap, showing that the process of sparging avoids low oxygen levels that inhibit copper extraction.

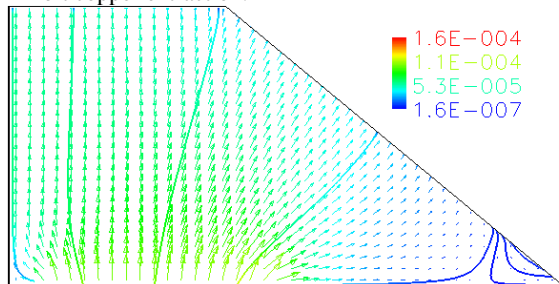


**Figure 2:** Streamlines with vector plot and coloured by speed,  $V_{in}=1.0 \times 10^{-4}$ ,  $q_l=0.5q_{L,0}$ ,  $K=5 \times 10^{-10}$

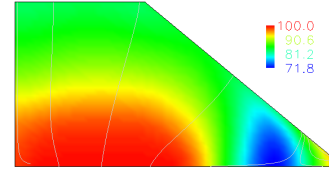


**Figure 3:** Streamlines with contours of normalised mass fraction oxygen % ( $100 \times W_o/0.22$ ),  $V_{in}=1.0 \times 10^{-4}$ ,  $q_l=0.5q_{L,0}$ ,  $K=5 \times 10^{-10}$

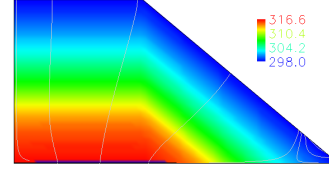


**Figure 4:** Streamlines with contours of  $T$ ,  $V_{in}=1.0 \times 10^{-4}$ ,  $q_l=0.5q_{L,0}$ ,  $K=5 \times 10^{-10}$

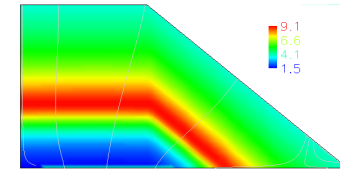


**Figure 5:** Streamlines with contours of  $100 \times \alpha$  (1 year),  $V_{in}=1.0 \times 10^{-4}$ ,  $q_l=0.5q_{L,0}$ ,  $K=5 \times 10^{-10}$

In Figure 3, the minimum oxygen level occurs near the bottom right hand corner of the heap, which is caused by the low flow rates (Figure 2) in that area. This low oxygenated area occurs in spite of the fact there is some natural convection in that area. In Figure 4 and 5 the temperature and copper extraction (after 1 year) are shown revealing the strong dependence of the copper extraction upon the temperature.

In Figures 6 and 7 a comparison is made between cases with and without sparging, for fixed liquid flow rate, bacterial concentration and permeability. Figure 7 shows that oxygen becomes depleted without the use of sparging, limiting copper extraction with a characteristic extraction time of 13,258 days, compared to 8,013 days when sparging at  $V_{in}=1 \times 10^{-4}$  (Figure 6).

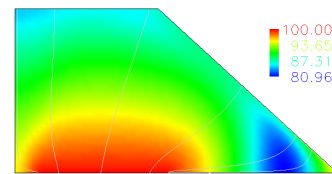


**Figure 6:** Streamlines with contours of normalised oxygen mass fraction oxygen % ( $100 \times W_o/0.22$ ),  $V_{in}=1 \times 10^{-4}$ ,  $q_l=1.5q_{L,0}$ ,  $K=5 \times 10^{-10}$

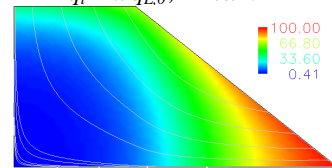


**Figure 7:** Streamlines with contours of normalised oxygen mass fraction oxygen % ( $100 \times W_o/0.22$ ), no sparging,  $q_l=1.5q_{L,0}$ ,  $K=5 \times 10^{-10}$

In Table 2 a comparison of the characteristic copper extraction time  $t_* \equiv 1/(d\alpha/dt)$  is made for different flow rates, showing that  $t_*$  is highly dependent on the liquid flow rate, with a minimum occurring around  $0.5q_{L,0}$  where  $q_{L,0}=1.4 \times 10^{-6}$ . This dependence occurs due to the cooling effect the liquid has on the air. Thus liquid flow rate may be used to control the temperature distribution to ensure that it remains as close as possible to the optimal value of around 311K.

$q_L (x q_{L,0})$	$t_* (\text{days})$
0.125	17857
0.25	10371
0.5	6667
1	7042
1.5	8013
2	8264
3	8333

**Table 2:**  $t_*$  versus liquid flow rate  $q_L (x q_{L,0})$ ,  $K=5 \times 10^{-10}$ ,  $V_{in}=1 \times 10^{-4}$

In Table 3 the effect of the permeability is shown on the characteristic copper extraction time  $t_*$ . It is only dependent on the permeability to a small extent for an air sparging velocity  $V_{in}=1.0 \times 10^{-4}$  and  $V_{in}=1.0 \times 10^{-5}$ , as explained by the  $t_*$  ratio in Table 3. The relative difference is negligible in terms of long term extraction.

$K$	$t_* (\text{days})$		$t_* \text{ ratio}$
	$V_{in}=1.0 \times 10^{-4}$	$V_{in}=1.0 \times 10^{-5}$	
$5 \times 10^{-9}$	8065	8170	0.9871
$5 \times 10^{-10}$	8013	8621	0.9295
$5 \times 10^{-11}$	8091	8681	0.9320

**Table 3:**  $t_*$  versus  $K$  for  $q_L=1.5q_{L,0}$ , and associated  $t_*$  ratio of  $V_{in}=1.0 \times 10^{-5}$  to  $V_{in}=1.0 \times 10^{-4}$

### High Bacterial Levels

In this section we look at the results in the case of a higher constant bacterial concentration,  $X=5 \times 10^{13}$  bacteria/m<sup>3</sup>, compared to the last section where  $X=5 \times 10^{12}$ . One of the most significant changes was the decrease in characteristic copper extraction time  $t_*$  (compare Table 2 and Table 4). Again, the liquid flow rate has a substantial effect on the copper extraction (see Table 4), due to the ability of the liquid to cool the heap, and push the temperature closer to the optimal temperature ( $\sim 311K$ ). Table 4 shows the best liquid flow rate occurs around  $5q_{L,0}$ , and such estimates could be useful in practice. The computed results for this “optimal” liquid flow rate are shown in Figures 8-11. Figure 8 shows some entrainment of air occurs into the heap, whilst in Figure 9 we see the oxygen mass fraction becomes depleted well before air leaves the heap, suggesting that a higher inlet velocity should be used (see Figures 12-14). Figure 10 shows that the temperature is distributed around the optimal temperature of 311K for a large area, leading to extraction in some areas as high as 92% after one year.

$q_L (x q_{L,0})$	$t_* (\text{days})$
1	2274
2	1409
3	1140
4	1122
5	1119
6	1125

**Table 4:**  $t_*$  versus liquid flow rate  $q_L (x q_{L,0})$ ,  $V_{in}=1 \times 10^{-4}$ ,  $K=5 \times 10^{-10}$

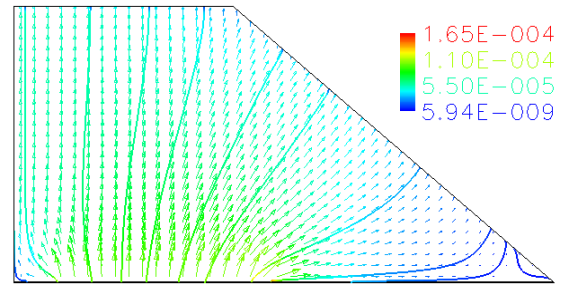


**Figure 8:** Streamlines with vector plot and coloured by speed,  $V_{in}=1.0 \times 10^{-4}$ ,  $q_L=5q_{L,0}$ ,  $K=5 \times 10^{-10}$

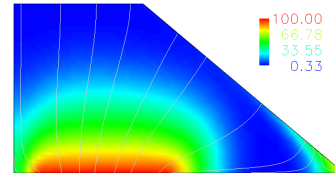


**Figure 9:** Streamlines with contours of normalised oxygen mass fraction % ( $100 \times W_o/0.22$ ),  $V_{in}=1.0 \times 10^{-4}$ ,  $q_L=5q_{L,0}$ ,  $K=5 \times 10^{-10}$

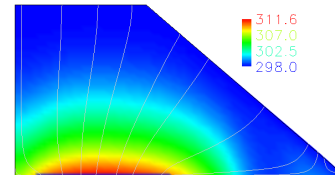


**Figure 10:** Streamlines with contours of  $T$ ,  $V_{in}=1.0 \times 10^{-4}$ ,  $q_L=5q_{L,0}$ ,  $K=5 \times 10^{-10}$

This estimate does not represent an extraction value obtainable in practice, since we have not accounted for variation in  $FPY$  as discussed earlier. Further work will be required to account for this. Overall the predicted characteristic extraction time  $t_*$  is 1119 days (see Table 4).

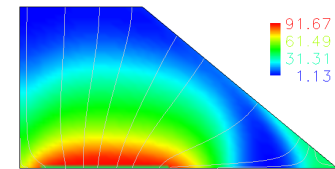


**Figure 11:** Streamlines with contours of  $100 \times \alpha (1 \text{ year})$ ,  $V_{in}=1.0 \times 10^{-4}$ ,  $q_L=5q_{L,0}$ ,  $K=5 \times 10^{-10}$

Figure 14 shows that for a higher inlet velocity of  $V_{in}=1.0 \times 10^{-3}$ , a completely different copper extraction profile is obtained, with most of the extraction occurring in the middle of the bed. This suggests the possibility of controlling copper extraction through different regions of the bed, by using certain combinations of liquid and air flow rates. This higher air velocity pushes the characteristic copper extraction time down to 676 days (see Table 5), since more oxygen is present in the heap (Figure 12) and the temperature distribution is closer to the optimal value of 311K (Figure 13). An even higher sparging velocity of  $V_{in}=1 \times 10^{-2}$  does not provide any better copper extraction (see Table 5), because the temperature becomes higher than optimal over a large region.

For the permeability  $K=5 \times 10^{-10}$ , the characteristic copper extraction time ratio (see Table 6) depends in the inlet velocity, but the dependence is less for  $K=5 \times 10^{-9}$ . This

comparison shows that if the heap permeability can be increased to  $K=5 \times 10^9$ , a lower sparging rate can be used to obtain similar copper extraction. In fact, a characteristic copper extraction time without sparging and  $K=5 \times 10^9$  has been found to be 2,212 days, indicating that for the size of heap studied here, there is essentially no benefit to be gained from sparging with such high permeabilities. This analysis shows the benefits of creating high permeability, to reduce costs of sparging.

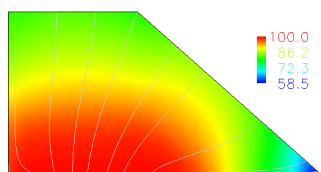


**Figure 12:** Streamlines with contours of normalised mass fraction oxygen %, ( $100 \times W_o/0.22$ ),  $V_{in}=1.0 \times 10^{-3}$ ,  $q_l=5q_{L,0}$ ,  $K=5 \times 10^{10}$

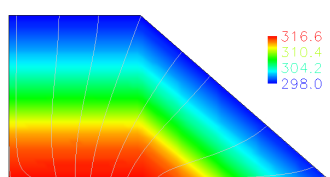


**Figure 13:** Streamlines with contours of  $T$ ,  $V_{in}=1.0 \times 10^{-3}$ ,  $q_l=5q_{L,0}$ ,  $K=5 \times 10^{10}$

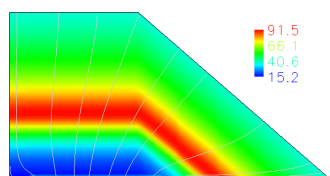


**Figure 14:** Streamlines with contours of copper extracted  $100x\alpha$  (after 1 year),  $V_{in}=1.0 \times 10^{-3}$ ,  $q_l=5q_{L,0}$ ,  $K=5 \times 10^{10}$

$V_{in}$	$t_*$ (days)
$1 \times 10^{-2}$	694
$1 \times 10^{-3}$	676
$1 \times 10^{-4}$	1119

**Table 5:**  $t_*$  versus  $V_{in}$  for  $K$  for  $q_L=5q_{L,0}$

$K$	$t_*$ (days)		$t_*$ ratio
	$V_{in}=1 \times 10^{-4}$	$V_{in}=1 \times 10^{-5}$	
$5 \times 10^{-9}$	2217	2212	1.002
$5 \times 10^{-10}$	2274	3155	0.7208

**Table 6:**  $t_*$  for  $q_L=1q_{L,0}$ , and associated ratio of  $t_*$  for  $V_{in}=1.0 \times 10^{-5}$  to  $V_{in}=1.0 \times 10^{-4}$

## CONCLUSION

The model simulation presented in this work has shown that air sparging has a critical effect on the heap leaching process, in addition to the effect of the liquid flow rate. This is the first time this effect has been simulated in a numerical model. Copper extraction has been shown to increase greatly with the use of sparging, in comparison to relying on natural convection. However, where the oxygen was kept at high levels, one must be cautious about the copper extraction values, since other factors are likely to become rate limiting, such as liquid flow. The ability to determine optimal air and liquid flow rates was illustrated, and this ability could be of use in practice. The ability to control copper extraction in particular parts of the bed was

shown, which also could be of interest to operators. It has been shown that for permeabilities as large as  $K=10^9$ , one does not achieve any better copper extraction by sparging. Other interesting aspects for further work include investigating cooler ambient temperatures and its effect on bed temperature and air entrainment. It may also be possible to turn off sparging (at least temporarily) once heap temperatures become high enough to allow natural convection to take over, thus saving the cost of sparging. The model presented can be improved by including these aspects and by relaxing the simplifications in the model of liquid flow, bacterial growth and ratio of pyrite to chalcocite leached ( $FPY$ ). The effect of heap dimensions could also be investigated with regard to many of the aspects mentioned in this work.

## ACKNOWLEDGMENTS

The help of Jakub Bujalski and Peter Witt on several issues were greatly appreciated. Funding from APA and a CSIRO top-up scholarship was greatly appreciated.

## REFERENCES

- AHONEN, L. and TUOVINEN, O.H., (1989), "Microbiological oxidation of ferrous iron at low temperatures", *Appl. Environ. Microbiol.*, **55**(2), 312-316.
- AL-KHLAIFAT, A. and ARASTOPOUR, H. (1997), "Simulation of two-phase flow through low-permeability porous media", AEA technology international user conference '97.
- BARTLETT, R., (1998), "Solution Mining: Leaching and fluid recovery of materials, 2<sup>nd</sup> edition", The Netherlands: Gordon and Breach Science Publishers.
- BARTLETT, R. and PRISBREY, K.A. (1996), "Convection and diffusion limitation aeration during biooxidation of shallow ore heaps", *Int. J. Miner. Process.*, **47**, 75-91.
- BEAR, J., (1972), "Dynamics of fluids in porous media", American Elsevier Science Publishing Co. Inc.
- BOUFFARD, S.C. and DIXON, D. (2001), "Investigative study into the hydrodynamics heap leaching processes", *Met. Mat. Trans.*, **32B**, 899-909.
- CASAS, J.M., MARTINEZ, J., MORENO, L., and VARGOS, T., (1998), "Bioleaching model of a copper-sulphide ore bed in heap and dump configurations", *Met. Mat. Trans.*, **29B**, 899-909.
- LU, N. and ZHANG, Y., (1997), "Onset of thermally induced air convection in mine wastes", *Int. J. Heat Mass Transfer*, **40** (11), 2621-2636.
- PANTELIS, G. and RITCHIE, A.I.M., (1991), "Rate-limiting factors in dump leaching of pyritic ores", *Appl. Math. Modelling*, **16**, 553-560.
- PANTELIS, G. and RITCHIE, A.I.M., (1992), "Macroscopic transport mechanisms as a rate-limiting factor in dump leaching of pyritic ores", *Appl. Math. Modelling*, **15**, 136-143.
- PANTELIS, G., RITCHIE, A.I.M. and STEPANYANTS, Y.A. (2002), "A conceptual model for the description of oxidation and transport process in sulphidic waste rock dumps", *Appl. Math. Modelling*, **26** (2), 751-770.
- PERRY, J.H. and GREEN, D.W., (1984), "Perry's Chemical Engineers' Handbook, 6<sup>th</sup> edition", McGraw-Hill Book Company, Japan.